2008 SCEC ANNUAL REPORT

STRESS UNCERTAINTIES OF THE SAN ANDREAS FAULT SYSTEM DUE TO VARIATIONS IN SLIP RATES, FAULT LOCKING DEPTHS, AND FAULT RHEOLOGY.

FUNDED PROPOSALS RELATED TO THIS PROJECT:

NSF CAREER ($501,048) 6/1/09 - 5/13/14: *CAREER: An integrated geologic, geodetic, and paleoseismic study of plate boundary stress evolution and geoscience education utilizing the EarthScope database*; PI = B. Smith-Konter.

NSF Tectonics ($232,299) 1/1/09 - 12/31/11: *Integrating geologic, geodetic, and coastal tide gauge observations with 100-year vertical deformation models of California earthquake history*; PI = B. Smith-Konter.

NASA EarthScope ($386,471) 12/15/08 - 12/14/11; *Geodetic imaging and modeling of the San Andreas Fault System*; PI = D. Sandwell (UC San Diego); Co-PI = B. Smith-Konter.

PUBLICATIONS AND ABSTRACTS RESULTING FROM THIS PROJECT:

Smith-Konter, B., and D.T. Sandwell, Stress evolution of the San Andreas Fault System: Recurrence interval versus locking depth, submitted to *Geophys. Res. Lett*, *in revision*.

Smith-Konter, B., T. Solis, and D.T. Sandwell (2008), Data-derived stress uncertainties of the San Andreas Fault System, *EOS Trans. AGU*, *89 (53)*, Fall Meet. Suppl., U51B-0029.

Smith-Konter, B., T. Solis, and D.T. Sandwell (2008), Stress evolution of the San Andreas Fault System: Hindcast stress accumulation models and stress rate uncertainties, *Proceedings from 7th U.S./Japan Natural Resources Panel for Earthquake Research.*

Smith-Konter, B., T. Solis, and D.T. Sandwell (2008), Stress uncertainties of the San Andreas Fault System, *Proceedings from the 2008 Southern California Earthquake Center Annual Meeting,* Volume XVIII.

Sandwell, D., B. Smith-Konter, and M. Wei (2008), Geodetic imaging of large-scale continental deformation with ALOS InSAR and CGPS, 2008 *GSA Joint Annual Meeting*, 204-6.

Sandwell, D., and B. Smith-Konter (2008), Imaging crustal deformation along the San Andreas Fault System with ALOS InSAR and GPS, 2008 *IGARSS Meeting*.

Smith-Konter, B. D.T. Sandwell, and T. Solis (2009), New locking depth estimates of the San Andreas Fault System derived from the PBO GPS network, *2009 EarthScope National Meeting*, Boise, ID.

Sandwell, D.T., P. Bird, A. Freed, C. Kreemer, T. Parsons, B. Smith-Konter, and S. Wdowinski (2009), Comparison of Strain-rate maps of Western North America, *2009 EarthScope National Meeting*, Boise, ID.

Wei, M., D. Sandwell, and B. Smith-Konter (2009), Optimal Combination of InSAR and GPS for measuring interseismic crustal deformation, *2009 EarthScope National Meeting*, Boise, ID.

Solis, T., and B. Smith-Konter (2009), Investigating active fault segment locations of the San Andreas Fault System using high-resolution LIDAR data and the SCEC Community Fault Model, *UTEP Geological Sciences 23rd Annual Student Research Colloquium*.

Solis, T., and B. Smith-Konter (2009), Investigating active fault segment locations of the San Andreas Fault System using high-resolution LIDAR data and the SCEC Community Fault Model, *2009 SACNAS Meeting*.

SCEC funding this past year supported a sensitivity analysis of stress models based on variations in model parameters (locking depth, slip rate, coefficient of friction, mantle viscosity, elastic plate thickness) and earthquake slip history. To explore stress variations of the San Andreas Fault System (SAFS) throughout the earthquake cycle, present-day model constraints were placed using the contemporary GPS velocity field [e.g., *McClusky et al*., 2001; *Shen et al*., 2003], while paleoseismic & historical seismicity data, combined with geologic slip rates [*WGCEP*, 1995 2003; 2007], were used to prescribe coseismic slip histories spanning the last 1000 years [*Smith and Sandwell*, 2006; 2009].

For this project, we established three primary research tasks:

- *Explore the uncertainties in secular stress rate by calculating Coulomb stress rate derivatives with respect to published estimates of slip rates, locking depths, and coefficients of friction.*
- *Explore the uncertainties in the present-day stress field by calculating Coulomb stress accumulation derivatives with respect to variations in slip history, elastic plate thickness, and mantle viscosity.*
- *Perform a new investigation of fault locking depths with varied slip scenarios for the 35$^+$ fault segments that comprise the latest version of our model, which will also incorporate updated fault geometry using the SCEC Community Fault Model.*

Subsequently, the focus of this research has been 1) to investigate secular stress rates of the SAFS, 2) to investigate conditions of the present-day stress field, and 3) to develop an improved model of time-dependent stress accumulation and relaxation reflecting 1000 years of SAFS earthquake activity. Four primary findings have resulted from this work, and form the basis of future research:

1) Modeled Coulomb stress accumulation rates range from 0.5-7 MPa/100 years (Fig.1a), vary as a function of fault locking depth, slip rate, and fault geometry, and are inversely proportional to earthquake recurrence intervals (20-500 years).
2) Stress accumulation rate uncertainties, derived from a range of geodetically- and seismically-derived locking depth estimates, are roughly +3/-0.5 MPa/100 years (Fig. 1b); uncertainties derived from realistic slip rate variations are roughly +1/-0.5 MPa/100 years.
3) Calculations of accumulated stress over several earthquake cycles are consistent with coseismic stress drops of ~ 3-8 MPa (Fig. 1c), however such calculations

depend largely on the rupture history of the fault [e.g., *Grant and Lettis*, 2002; *Weldon et al.*, 2004] over the past few thousand years. Uncertainties in stress accumulation can range from 0.5-3.0 MPa (Fig. 1d) for various slip history scenarios.

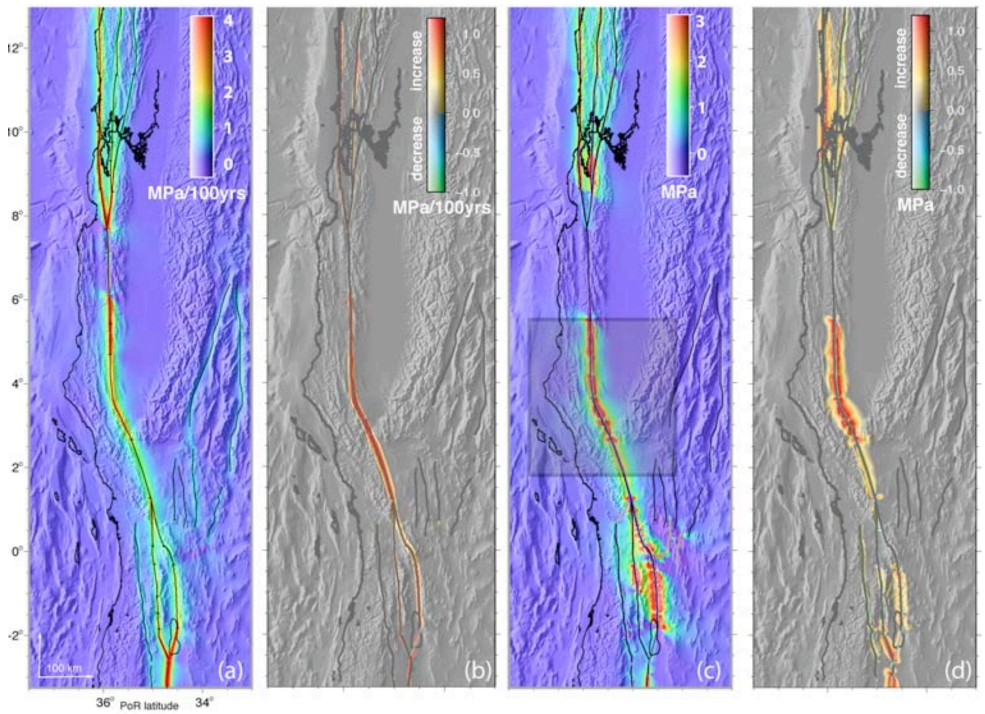

Fig. 1. **(a)** Coulomb stress accumulation rate of the SAFS, modified from *Smith and Sandwell* [2003]. Color scale is saturated at 4 MPa/100yrs. **(b)** Stress accumulation rate uncertainty calculated from (a) (fault depths ranging from 5-26 km) and a model using system-wide locking depths that are decreased by 50%. Color scale is saturated at ± 1 MPa/100 yrs. **(c)** Present-day (calendar year 2008) stress accumulation based on 75 historical and prehistorical earthquake ruptures modified from *Smith and Sandwell* [2006]. Color scale is saturated at 3 MPa. Shaded box represents location of Carrizo section, which we plan to further study as a case example of stress variations generated by new paleoseismic results **(d)** Present-day **(**2008) stress accumulation uncertainty calculated from (c) and a model using system-wide slip histories that relieve 70% of their respective slip deficits (~0.1-3.0 m). Color scale is saturated at ± 1 MPa.

4) To prepare for a new fault locking depth analysis using the EarthScope and SCEC GPS array, we conducted a small investigation of fault locations and geometries provided by the SCEC Community Fault Model (CFM), our initial model segments, and the B4 LIDAR data. Our initial model segments are in good agreement with the SCEC CFM, matching to within ~ 1-2 km of the CFM database. Comparison of the CFM to the B4 data yielded a few surprising results; while some CFM locations match the B4 data to within 0.1 km, several CFM locations were found to deviate from the B4 data by over 1 km (Fig 2.). We are currently revisiting these anomalous regions to further investigate the source of the geo-location errors. We have subsequently refined our model fault segments to match the B4 data to the best of our ability, and have also added additional fault segments in the Eastern California

Shear Zone and Mojave Desert using the CFM database. We have begun the fault locking depth analysis, and plan to report our results at the 2009 EarthScope National Meeting in Boise, ID in May.

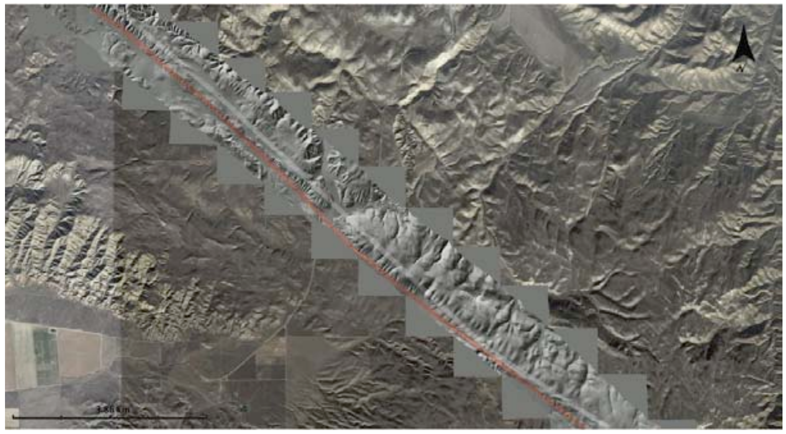

Fig. 2. Zoomed Google Earth view of B4 LIDAR data segment near the Big Bend region of the San Andreas fault. LIDAR data surface expression is shown in grey. White line represents SCEC CFM fault location. Red line represents digitized fault trace based on the LIDAR imagery. Here we measure an average location variation of 0.43 km.

Our models show that Coulomb stress accumulation rate of the SAFS is primarily dependent on slip rates and locking depths that are determined by interseismic GPS velocities; these stress rates do not strongly depend on a prescribed earthquake history, nor are they sensitive to viscoelastic rheology. For example, a 25% reduction in elastic plate thickness generates modeled stress rates that decrease by less than 0.1 MPa/100 years. Comparable variations in frictional coefficients yield similar results. While we believe that stress accumulation rate estimates are fairly robust, we have begun work to compare interseismic stress rates in Western North America with those provided by models and data interpolations of other colleagues (A. Freed, P. Bird, C. Kreemer, T. Parsons, S. Wdowinski, and F. Pollitz). Preliminary results with Freed's stress models [*Freed et al.*, 2007] of southern California suggest that our peak stress rates are in general

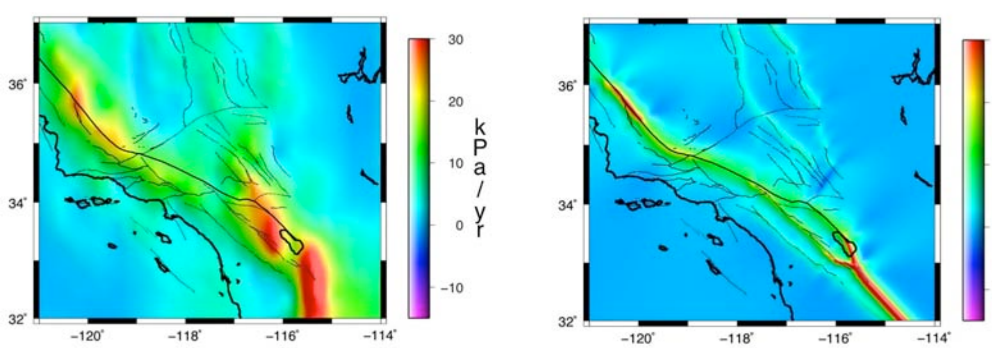

(a) **(b)**

Fig 3. (a) Interseismic Coulomb stress rate resolved onto vertical right-lateral strike slip faults parallel to the SAF after *Freed et al*. [2007]. **(b)** Interseismic Coulomb stress rate resolved onto vertical right-lateral strike slip faults from *Smith and Sandwell* [2003; 2009] with faults added in the Mojave desert and Eastern California Shear Zone. Note that units are kPa/yr or 0.1 MPa/100yr.

agreement, however our rates are lower in magnitude in some regions and more concentrated near the active faults (Fig. 3). Part of this could be due to the fact that the spatial density of the GPS velocity points is not sufficient to resolve scales less than about 50 km in some places. Results of a more comprehensive analysis will be presented at the 2009 EarthScope National Meeting in Boise, ID.

Estimates of Coulomb stress evolution on fault segments spanning multiple earthquake cycles, however, are highly dependent on the prescribed slip history of each fault segment. Among several analyses of stress rate uncertainty, we have found, for example, that when 30% of the known historic slip deficit remains unaccounted for in our models, stress uncertainties of 3 MPa are possible. Stress variations of these magnitudes have critical implications for seismic hazard analyses given that modeled stress accumulation levels of the southern San Andreas appear to be approaching those of historically great events ($\sim 7^+$ MPa) (Fig. 1c). In addition, we also investigated possible improvements to our rupture scenario based on SCEC community suggestions. Modifications in rupture length of the 1857 San Andreas event (i.e, extending the rupture south through the Cajon Pass) produced a decrease in modeled stress accumulation by 1 MPa along the southern San Andreas (San Bernardino) segment.

Freed, A. M., S. T. Ali, and R. Bürgmann (2007), Evolution of stress in southern California for the past 200 years from coseismic, postseismic, and interseismic processes, *Geophys. J. Inter.*, 169, 1164-1179.

Grant., L. B. and W. R. Lettis (2002), Introduction to the Special Issue on Paleoseismology of the San Andreas Fault System, *Bull. Seis. Soc. Amer*., 92, 2552-2554.

McClusky, S., S.C. Bjornstad, B.H. Hager, R.W. King, B.J. Meade, M.M. Miller, F.C. Monastero, and B.J. Souter (2001), Present day kinematics of the Eastern California Shear Zone from a geodetically constrained block model, *Geophys. Res. Lett*., 28, 3369-3372.

Shen, Z.K., D.C. Agnew, and R.W. King (2003), The SCEC Crustal Motion Map, Version 3.0, http://epicenter.usc.edu/cmm3.

Smith, B., and D. T. Sandwell (2004), A 3-D semi-analytic viscoelastic model for time-dependent analysis of the earthquake cycle, *J. Geophys. Res*., doi:10.1029/2004JB003185.

Smith, B., and D. T. Sandwell (2006), A model of the earthquake cycle along the San Andreas Fault System for the past 1000 years, *J. Geophys. Res*., 111, doi:10.1029/2005JB003703.

Smith-Konter, B., and D. T. Sandwell (2009), Stress evolution of the San Andreas Fault System: recurrence interval versus locking depth, *submitted to GRL*, in revision.

Weldon, R., T. Fumal, and G. Biasi (2004), Wrightwood and the earthquake cycle: What a long recurrence record tells us about how faults work, *GSA Today*, 14, doi:10.1130/1052-5173.

Weldon, R. T. Fumal, G. Biasi, and K. Scharer (2005), Past and future earthquakes on the San Andreas fault, *Science*, 308, doi: 10.1126/science.1111707.

Working Group on California Earthquake Probabilities (WGCEP) (1995), Seismic hazards in southern California: Probable earthquakes, 1994 to 2024, Bull. Seis. Soc. Amer. 85, 379-439.

Working Group on California Earthquake Probabilities (WGCEP) (2003), Earthquake probabilities in the San Francisco Bay region: 2002-2031, *U.S. Geol. Surv. Open File Rep.*, 03-214.

Working Group on California Earthquake Probabilities (WGCEP) (2007), The Uniform California Earthquake Rupture Forecast, Version 2 (UCERF 2), *U.S. Geol. Surv. Open File Rep.*, 2007-1473.